Tetrasubstituted Guanidinate Anions as Supporting Ligands in Organoyttrium Chemistry

Zhiping Lu,† Glenn P. A. Yap, and Darrin S. Richeson*

Department of Chemistry, University of Ottawa, Ottawa, Ontario, Canada K1N 6N5

Received October 23, 2000

Addition of $N(SiMe_3)_2$ anion equivalents to $^iPrN{=}C{=}N^iPr$ followed by reaction with YCl_3 generated the dimeric complex $\{[(Me_3Si)_2NC(N^iPr)_2]_2Y(\mu\text{-}Cl)\}_2$ (**2**). Complex **2** has proven to be an excellent starting material for preparation of a series of hydrocarbyl and amido products, $[(Me_3Si)_2NC(N^iPr)_2]_2YCH(SiMe_3)_2$ (**3**), $[(Me_3Si)_2NC(N^iPr)_2]_2YN(SiMe_3)_2$ (**4**), $[(Me_3Si)_2NC(N^iPr)_2]_2Y(\mu\text{-}Me)_2Li[Me_2NCH_2CH_2NMe_2]$ (**5**), and $[(Me_3Si)_2NC(N^iPr)_2]_2YC(CH_3)_3$ (**6**). Definitive evidence for the molecular structures of **2**, **3**, **5**, and **6** is provided through single-crystal X-ray analyses, which are presented. These results provide the first reported examples of organoyttrium complexes supported by a guanidinate ligand.

Introduction

Substituted guanidinate anions, $[RNC(NR'_2)NR'']^-$, represent appealing and flexible supporting ligands for a variety of metal complexes. Recent interest in the ligating properties of these species has led to preparation and characterization of metal complexes from across the periodic table.[1] These ligands fall into a family of bidentate, three-atom-bridging ligands with the general formula $RNXNR^-$ (X = CNR'_2[2], CR',[3] or N).[4] One member of this family, *N*,*N*′-bis(trimethylsilyl)-benzamidinate-based ligands $[Me_3SiNC(C_6H_{5-n}R_n)NSiMe_3]^-$, has recently been employed for preparation of inorganic complexes of the lanthanide elements[5] and organometallic complexes of yttrium.[6] In contrast, the application of guanidinate ligands in lanthanide or group 3 chemistry has been restricted to a single report.[7] Variation of the organic substituents on the nitrogen atoms of the guanidinates should allow for rational modifications to both the steric bulk and electronic properties of the supporting ligands.

In this contribution we report the first guanidinate complexes of Y. The bis(guanidinate) complex $[(Me_3Si)_2NC(N^iPr)_2]_2Y(\mu\text{-}Cl)\}_2$ can be conveniently prepared and is shown to be a useful starting material for entry to hydrocarbyl and amido complexes that possess the guanidinate ligand scaffold. The structural features of several members of this new family of complexes are reported.

Results and Discussion

Synthesis of Bis(guanidinate) Yttrium Chloro, Amido, and Hydrocarbyl Complexes. The lithium salt of *N*,*N*′-diisopropyl-*N*″-bis(trimethylsilyl)guanidinate anion, **1**, can be generated by the direct reaction of *N*,*N*′-diisopropylcarbodiimide ($^iPrN{=}C{=}N^iPr$) with 1 equiv of $LiN(SiMe_3)_2$ in diethyl ether. While **1** could be isolated in pure form by simple removal of the solvent, in most cases freshly prepared solutions of lithium guanidinate can be used in metathesis reactions with metal halides.[8] For example, addition of 0.5 equiv of anhydrous YCl_3 to a solution of in situ prepared **1** followed by recrystallization resulted in isolation of the neutral solvent-free dinuclear guanidinate complex

† Present location: Department of Chemistry, Central China Normal University, Wuhan, Hubei, People's Republic of China, 430079.

(1) For examples of complexes with monoanionic guanidinate ligands see: Bailey, P. J.; Grant, K. J.; Mitchell, L. A.; Pace, S.; Parkin, A.; Parsons, S. *J. Chem. Soc., Dalton Trans.* **2000**, 1887. Giesbracht, G. R.; Whitener, G. D.; Arnold, J. *Organometallics* **2000**, *19*, 2809. Foley, S. R.; Yap, G. P. A.; Richeson, D. S. *J. Chem. Soc., Chem. Commun.* **2000**, 1515. Thirupathi, N.; Yap, G. P. A.; Richeson, D. S. *Organometallics* **2000**, *19*, 2573. Thirupathi, N.; Yap, G. P. A.; Richeson, D. S. *J. Chem. Soc., Chem. Commun.* **1999**, 2483. Tin, M. K. T.; Thirupathi, N.; Yap, G. P. A.; Richeson, D. S. *J. Chem. Soc., Dalton Trans.* **1999**, *17*, 2947. Tin, M. K. T.; Yap, G. P. A.; Richeson, D. S. *Inorg. Chem.* **1999**, *38*, 998. Giesbracht, G. R.; Shafir, A.; Arnold, J. *Dalton Trans.* **1999**, 3601. Decams, J. M.; Pfalzgraf, L. G. H.; Vaisserman, J. *Polyhedron* **1999**, 2483. Aelits, S. L.; Coles, M. P.; Swenson, D. G.; Jordan, R. F.; Young, V. G. *Organometallics* **1998**, *17*, 3265. Chivers, T.; Parvez, M.; Schatte, G. *J. Organomet. Chem.* **1998**, *550*, 213. da S. Maia, J. R.; Gazard, P. A.; Kilner, M.; Batsanova, A. S.; Howard, J. A. K. *J. Chem. Soc., Dalton Trans.* **1997**, 4625. Robinson, S. D.; Sahajpal, A. *J. Chem. Soc., Dalton Trans.* **1997**, 3349. Bailey, P. J.; Bone, S. F.; Mitchell, L. A.; Parsons, S.; Taylor, K. J.; Yellowlees, L. J. *Inorg. Chem.* **1997**, *36*, 867. Bailey, P. J.; Mitchell, L. A.; Parsons, S. *J. Chem. Soc., Dalton Trans.* **1996**, 2839. Yip, H.-K.; Che, C.-M.; Zhou, Z.-Y.; Mak, T. C. W. *J. Chem. Soc., Chem. Commun.* **1992**, 1369.

(2) Mehrotra, R. C. In *Comprehensive Coordination Chemistry*; Wilkinson, G., Gillard, R. D., McCleverty, J. A., Eds.; Pergamon Press: Oxford, U.K., 1987; Chapter 13.8.

(3) Edelmann, F. T. *Coord. Chem. Rev.* **1994**, *137*, 403. Kilner, M.; Baker, J. *Coord. Chem. Rev.* **1994**, *133*, 219.

(4) Moore, D. S.; Robinson, S. D. *Adv. Inorg. Chem. Radiochem.* **1986**, *30*, 1.

(5) (a) Hagen, C.; Reddmann, H.; Amberger, H.-D.; Edelmann, F. T.; Pegelow, U.; Shalimoff, G. V.; Edelstein, N. M. *J. Organomet. Chem.* **1993**, *462*, 69. (b) Wedler, M.; Knosel, F.; Pieper, U.; Stalke, D.; Edelmann, F. T.; Amberger, H.-D. *Chem. Ber.* **1992**, *125*, 2171. (c) Wedler, M.; Recknagel, A.; Gilje, J. W.; Noltemeyer, M.; Edelmann, F. T. *J. Organomet. Chem.* **1992**, *426*, 295. (d) Recknagel, A.; Knosel, F.; Gornitzka, H.; Noltemeyer, M.; Edelmann, F. T.; Behrens, U. *J. Organomet. Chem.* **1991**, *417*, 363. (e) Wedler, M.; Noltemeyer, M.; Pieper, U.; Schmidt, H.-G.; Stalke, D.; Edelmann, F. T. *Angew. Chem., Int. Ed. Engl.* **1990**, *29*, 894.

(6) (a) Duchateau, R.; van Wee, C. T.; Meetsma, A.; van Duijnen, P. T.; Teuben, J. H. *Organometallics* **1996**, *15*, 2279. (b) Duchateau, R.; Meetsma, A.; Teuben, J. H. *Organometallics* **1996**, *15*, 1656. (c) Duchateau, R.; van Wee, C. T.; Teuben, J. H. *Organometallics* **1996**, *15*, 2291. (d) Duchateau, R.; van Wee, C. T.; Meetsma, A.; Teuben, J. H. *J. Am. Chem. Soc.* **1993**, *115*, 4931.

(7) Zhou, Y.; Yap, G. P. A.; Richeson, D. S. *Organometallics* **1998**, *17*, 4387.

(8) Wood, D.; Yap, G. P. A.; Richeson, D. S. *Inorg. Chem.* **1999**, *38*, 5788.

10.1021/om0009029 CCC: $20.00
Publication on Web 01/16/2001

Scheme 1

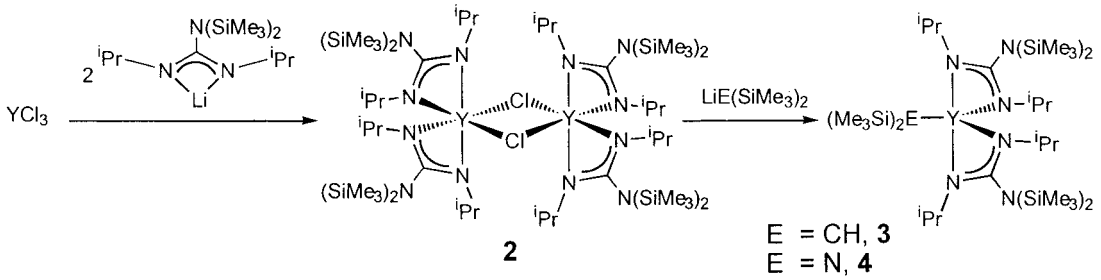

2

Scheme 2

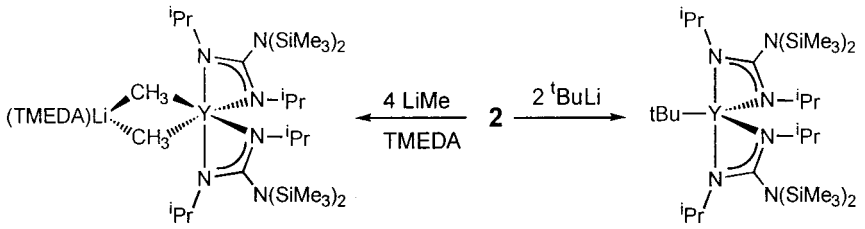

5 **6**

$\{[(Me_3Si)_2NC(N^iPr)_2]Y(\mu\text{-}Cl)\}_2$, **2**, in 73% yield (Scheme 1). Crystals of compound **2** showed no sign of decomposition, as monitored by NMR spectra, after more than six months when stored in a drybox. However, exposure of solid **2** to air led to a rapid change from colorless to deep brown with obvious deliquescence.

Notable ^1H and ^{13}C NMR spectroscopic features for **2** include the appearance of two sets of resonances of equal intensity for the guanidinate ^{i}Pr substituents, while the two $Si(CH_3)_3$ moieties of the ligand appear as a singlet, albeit broadened relative to the related signal for the lithium salt. These NMR features, and the results of the crystallographic characterization described below, provide the structure of **2** shown in Scheme 1. The inequivalence of the two ^{i}Pr groups is consistent with the octahedral-based metal coordination geometry shown for compound **2**, with one signal arising from the two pseudoaxial groups while the other comes from the two pseudoequatorial located substituents.

The appearance of two different ^{i}Pr groups contrasts with earlier spectroscopic observations on guanidinate complexes of Sm, Yb, Zr, and Hf as well as the reported benzamidinate complexes of Y.[6–8] All of these previously reported species appear to exhibit fast fluxional behavior of the ligands at room temperature and display a single set of resonances for the substituents on the coordinated N atoms. Increasing the steric demands of an amidinate ligand or introducing bulkier substituents on the metal center has been shown to slow this fluxional averaging.[6a,8,9] The appearance of distinct ^{i}Pr groups for **2** suggests a more rigid coordination environment for this complex and is consistent with retention of a dinuclear structure in solution (vida infra).

Not surprisingly, when a similar reaction between **1** and YCl_3 is carried out in THF, the "ate" complex, $[(Me_3Si)_2NC(N^iPr)_2]Y(\mu\text{-}Cl)_2Li(THF)_2$, was isolated.[10] Thus far, subsequent reactions with this compound have led to what appear to be a mixture of products.

Complex **2** is an excellent precursor for preparation of stable and well-defined yttrium guanidinate compounds through simple metathesis reactions. For example, chloride replacement can be accomplished by reaction with $LiCH(SiMe_3)_2$ or $LiN(SiMe_3)_2$ to yield complexes **3** and **4** (Scheme 1). Unlike **2** the room-temperature ^1H and ^{13}C NMR spectra for **3** and **4** display a single resonance for the guanidinate ^{i}Pr substitutents, indicating an increased rate of fluxionality and consistent with a less rigid mononuclear species. The presence of the $CH(SiMe_3)_2$ group in **3** is supported by a broad singlet (δ −1.18 ppm) in the ^1H spectrum integrating as a single proton and a downfield signal for the α-carbon in the ^{13}C spectrum (δ 41.33 ppm) that is coupled to the Y center (J_{Y-C} = 33 Hz). This signal compares well with that of the related amidinate species $PhC(NSiMe_3)_2YCH(SiMe_3)_2$ (^1H, −0.94 ppm; ^{13}C, 43.5 ppm, J_{Y-C} = 30 Hz).[6a] For reference, the corresponding ^{13}C NMR signal in $Cp^*_2YCH(SiMe_3)_2$ appears at 25.2 ppm with a J_{Y-C} of 36.6 Hz.[11]

Well-defined alkyl products were also obtained from the reaction of **2** with MeLi and ^{t}BuLi. In the case of MeLi, our efforts to isolate a single product led to the reaction sequence shown in Scheme 2. Not surprisingly, in the case of a rather small methyl substituent the Lewis acidic Y(III) center appears to achieve added stabilization by formation of the "ate" complex $\{-[(SiMe_3)_2NC(N^iPr)_2]_2Y(\mu\text{-}Me)_2\}^-$ over generation of the solvent-free neutral species. Therefore, the reaction of **2** with MeLi gave the best results when carried out in a 1:4 ratio to generate this species. Addition of tetramethylethylenediamine (TMEDA) to the reaction mixture further stabilizes the complex by coordinating to the Li cation and yields $[(SiMe_3)_2NC(N^iPr)_2]_2Y(\mu\text{-}Me)_2Li(TMEDA)$ (**5**).[12] Similar yttrium complexes have been reported with the benzamidinate and pentamethylcyclopentadienyl ligand systems.[6a,b,13]

(9) Littke, A.; Sleiman, N.; Bensimon, C.; Yap, G.; Brown, S.; Richeson, D. *Organometallics* **1998**, *17*, 446. Zhou, Y.; Richeson, D. S. *Inorg. Chem.* **1997**, *36*, 501.

(10) Empirical formula: $C_{34}H_{80}Cl_2LiN_6O_2Si_4Y$, fw = 884.15, T = 203 K, λ = 0.71073 Å, space group = $P\bar{1}$, a = 9.972(2) Å, b = 14.961(3) Å, c = 18.301(3) Å, α = 75.385(17)°, β = 86.81(2)°, γ = 78.91(2)°, V = 2592.5(9) Å^3, Z = 2, R indices [$I > 2\sigma(I)$] = $R(F)$ = 0.0531, $wR(F)$ = 0.0996. A thermal ellipsoid plot is included in the Supporting Information.

(11) Den Haan, K. H.; de Boer, J. L.; Teuben, J. H.; Spek, A. L.; Kojic-Prodic, D.; Hays, G. R.; Huis, R. *Organometallics* **1986**, *5*, 1726

Table 1. Crystal Data for Compounds $[(Me_3Si)_2NC(N^iPr)_2]_2Y(\mu\text{-}Cl)\}_2$ (2), $[(Me_3Si)_2NC(N^iPr)_2]_2YCH(SiMe_3)_2$ (3), $[(Me_3Si)_2NC(N^iPr)_2]_2Y(\mu\text{-}Me)_2Li[Me_2NCH_2CH_2NMe_2]$ (5), and $[(Me_3Si)_2NC(N^iPr)_2]_2YC(CH_3)_3$ (6)

	2	3	5	6
empirical formula	$C_{52}H_{128}C_{l2}N_{12}Si_8Y_2$	$C_{33}H_{83}N_6Si_6Y$	$C_{34}H_{86}LiN_8Si_4Y$(solvent)	$C_{30}H_{73}N_6Si_4Y$
fw	1395.10	821.50	815.29	719.21
temp (K)	203(2)	203(2)	203(2)	203(2)
λ (Å)	0.71073	0.71073	0.71073 A	0.71073
space group	$Pca2_1$	$P2_1/c$	$P\bar{1}$	$Pna2(1)$
unit cell dimens				
a (Å)	21.034(2)	22.6891(19)	12.812(3)	18.228(4)
b (Å)	20.060(2)	10.8334(9)	13.933(3)	13.678(4)
c (Å)	18.983(2)	21.3807(18)	17.309(3)	34.896(9)
α (deg)			100.87(1)	
β (deg)		108.0090(10)	93.91(2)	
γ (deg)			108.36(1)	
volume (Å^3)	8010(1)	4997.9(7)	2853.0(9)	8700(4)
Z	4	4	2	8
density (Mg/m^3) (calcd)	1.157	1.092	0.988	1.098
abs coeff (mm^{-1})	1.665	1.337	1.134	1.476
R1[a]	0.0478	0.0454	0.0541	0.0646
wR2[b]	0.0958	0.0822	0.1402	0.0981

[a] $R1 = \sum||F_o| - |F_c||/\sum|F_o|$. [b] $wR2 = (\sum w(|F_o| - |F_c|)^2/\sum w|F_o|^2)^{1/2}$.

The observation of equivalent ^{i}Pr and $SiMe_3$ substituents for the guanidinate ligand in the NMR spectra of **5** indicates that this species is undergoing an exchange of axial and equatorial ligand positions on the NMR time scale. The ^{1}H and ^{13}C NMR signals for the methyl groups in **5** (^{1}H, δ −0.65 ppm; ^{13}C, δ 11.8 ppm) are similar to the reported benzamidinate-containing complexes, $[PhC(NSiMe_3)_2]_2Y(\mu\text{-}Me)_2Li(TMEDA)$ (^{1}H, δ −0.48 ppm; ^{13}C, δ 10.1 ppm) and $Cp^*[PhC(NSiMe_3)]Y(\mu\text{-}Me)_2Li(TMEDA)$ (^{1}H, δ −0.91 ppm; ^{13}C, δ 13.5 ppm), and, like these species, **5** displayed a broad ^{13}C signal with no resolvable yttrium coupling.[6a,b]

The reaction of **2** with ^{t}BuLi followed a different course (Scheme 2). In this case, 2 equiv of alkyllithium produced the neutral alkyl-substituted product, $[(SiMe_3)_2NC(N^iPr)_2]_2YCMe_3$ (**6**), in an isolated yield of 70%. Interestingly, **6** appears to be stereochemically rigid at room temperature, as indicated in both the ^{1}H and ^{13}C NMR spectra of this complex, which displayed two closely grouped sets of resonances of equal intensity for the isopropyl groups of the guanidinate ligand. Furthermore, the $SiMe_3$ substituents are also divided into two singlets of 1:1 intensity. An intense singlet for the ^{t}Bu methyl groups was observed at 1.36 ppm, and a signal at 39.9 ppm in the ^{13}C NMR spectrum that was coupled to yttrium ($^1J_{Y-C} = 46$ Hz) was assigned to the tertiary carbon of the butyl ligand.

Structural Characterization of 2, 3, 5, and 6. To provide complete structural information for these novel guanidinate species, single-crystal X-ray structural investigations were carried out on complexes **2**, **3**, **5**, and **6**. Details for these data collections can be found in Table 1.

Figure 1 and Table 2 provide a summary of the results of the structural analysis of complex **2**. The dinuclear structure of this complex consists of two edge-shared distorted octahedral moieties. Each of the Y centers is coordinated to two bridging chloride ligands and two chelating bidentate guanidinate ligands. The two Y centers and the two Cl atoms are coplanar and each Y

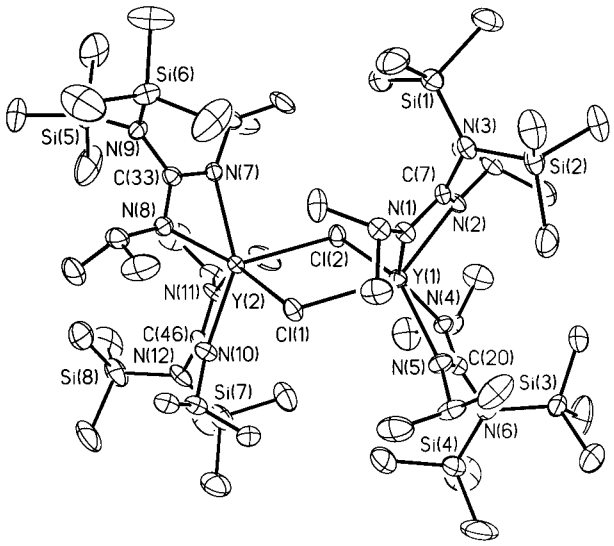

Figure 1. Molecular structure of $[(Me_3Si)_2NC(N^iPr)_2]_2Y(\mu\text{-}Cl)\}_2$ (**2**). Hydrogen atoms have been omitted for clarity. Thermal ellipsoids are drawn at 30% probability.

also lies in the CN_3 plane of the chelating guanidinate ligands. Within the chelating NCN unit the C−N distances are nearly equal (average C−N = 1.34 Å), indicating π electron delocalization within this unit.

For comparison with other guanidinate, amidinate, and cyclopentadienyl structures it is instructive to assign the guanidinate ligands as occupying a single coordination site defined by the central carbon of the CN_3 moieties. The angles defined by these centroids and the Y centers (C(7)−Y(1)−C(20) = 123.09(15)°; C(33)−Y(2)−C(46) = 122.17(17)°) are very similar to the analogous angles in the reported benzamidinate dimeric complexes.[6a,d]

As can be seen in Figure 1, the orientation of the $N(SiMe_3)_2$ groups relative to the NCNY plane is approximately perpendicular. This is an observation similar to that made for the reported Sm, Yb, and Zr complexes of this ligand family.[7,8] This disposition is likely the result of steric interactions between the ^{i}Pr functions and the bulky trimethylsilyl groups and eliminates the possibility of π overlap between these two moieties. However, this orientation of the bulky $N(SiMe_3)_2$

(12) Reaction of **2** and MeLi in a 1:2 ratio using diethyl ether as the reaction solvent produced the dinuclear complex $\{[(SiMe_3)_2NC(N^iPr)_2]_2Y(\mu\text{-}Me)\}_2$. Details of the synthesis, characterization, and reactivity of this species will appear in a future report.

Table 2. Selected Bond Distances [Å] and Angles [deg] for $[(Me_3Si)_2NC(N^iPr)_2]_2Y(\mu\text{-}Cl)\}_2$ (2)

Distances			
Y(1)−N(5)	2.326(4)	Y(2)−Cl(2)	2.7173(15)
Y(1)−N(2)	2.338(4)	Y(2)−Cl(1)	2.7253(15)
Y(1)−N(1)	2.384(4)	N(1)−C(7)	1.327(6)
Y(1)−N(4)	2.388(4)	N(2)−C(7)	1.344(6)
Y(1)−Cl(2)	2.7128(15)	N(3)−C(7)	1.421(7)
Y(1)−Cl(1)	2.7166(15)	N(4)−C(20)	1.329(7)
Y(1)−C(20)	2.788(6)	N(5)−C(20)	1.342(7)
Y(1)−C(7)	2.831(6)	N(6)−C(20)	1.439(7)

Angles			
N(5)−Y(1)−N(2)	113.69(16)	C(7)−N(2)−Y(1)	96.8(3)
N(5)−Y(1)−N(1)	104.04(15)	C(4)−N(2)−Y(1)	141.3(3)
N(2)−Y(1)−N(1)	55.95(14)	C(7)−N(3)−Si(1)	120.1(3)
N(5)−Y(1)−N(4)	57.06(15)	C(7)−N(3)−Si(2)	117.6(4)
N(2)−Y(1)−N(4)	103.21(15)	Si(1)−N(3)−Si(2)	122.3(3)
N(1)−Y(1)−N(4)	146.36(15)	C(20)−N(4)−C(14)	121.2(5)
N(5)−Y(1)−Cl(2)	135.10(12)	C(20)−N(4)−Y(1)	92.7(3)
N(2)−Y(1)−Cl(2)	99.15(11)	C(14)−N(4)−Y(1)	145.7(3)
N(1)−Y(1)−Cl(2)	119.86(11)	C(20)−N(5)−C(17)	121.2(5)
N(4)−Y(1)−Cl(2)	87.09(11)	C(20)−N(5)−Y(1)	95.2(3)
N(5)−Y(1)−Cl(1)	97.53(12)	C(17)−N(5)−Y(1)	143.7(4)
N(2)−Y(1)−Cl(1)	136.20(11)	C(20)−N(6)−Si(4)	120.2(4)
N(1)−Y(1)−Cl(1)	88.09(11)	C(20)−N(6)−Si(3)	117.3(4)
N(4)−Y(1)−Cl(1)	119.74(11)	Si(4)−N(6)−Si(3)	122.4(3)
Cl(2)−Y(1)−Cl(1)	76.30(4)	N(1)−C(7)−N(2)	112.1(5)
C(20)−Y(1)−C(7)	123.09(15)	N(1)−C(7)−N(3)	123.8(5)
Y(1)−Cl(1)−Y(2)	103.65(5)	N(2)−C(7)−N(3)	124.1(5)
Y(2)−Cl(2)−Y(1)	103.97(5)	N(3)−C(7)−Y(1)	178.8(4)
C(7)−N(1)−C(1)	121.2(5)	N(4)−C(20)−N(5)	115.0(5)
C(7)−N(1)−Y(1)	95.2(3)	N(4)−C(20)−N(6)	122.3(5)
C(1)−N(1)−Y(1)	143.3(3)	N(5)−C(20)−N(6)	122.6(5)
C(7)−N(2)−C(4)	121.6(4)	N(6)−C(20)−Y(1)	178.7(4)

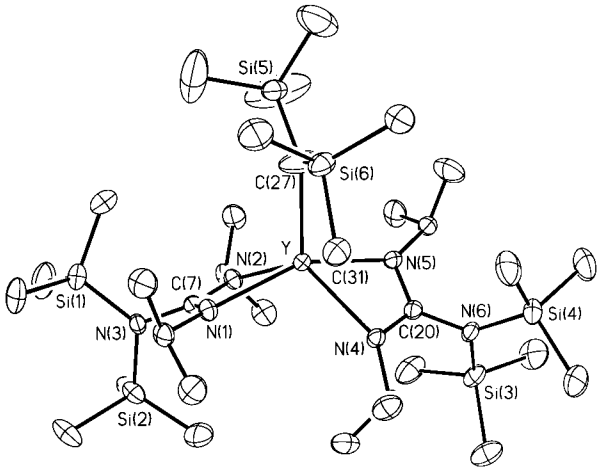

Figure 2. Molecular structure of $\{^iPrNC[N(SiMe_3)_2]N^i\text{-}Pr\}_2YCH(SiMe_3)_2$ (**3**). Hydrogen atoms have been omitted for clarity. Thermal ellipsoids are drawn at 30% probability.

group effectively adds steric bulk above and below the planar guanidinate ligand.

The structure of complex **3** is presented in Figures 2 and 3, with selected bond distance and angle data given in Table 3. Complex **3** can be compared with the only other structurally characterized guanidinate organolanthanoid complex, $[(SiMe_3)_2NC(N^iPr)_2]_2SmCH(SiMe_3)_2$,[7] and with the related benzamidinate complex $[p\text{-}MeOC_6H_4C(NSiMe_3)_2]_2YCH(SiMe_3)_2$.[6a] Like these compounds, the coordination geometry for the yttrium center of **3** can be described as trigonal planar by considering the ligand centroids defined by C(20), C(7), and the hydrocarbyl ligand C(27). Like **2**, the guanidinate ligands form a planar four-membered ring with the

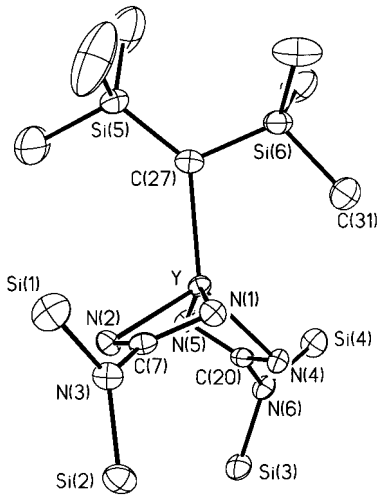

Figure 3. Alternative view of $\{^iPrNC[N(SiMe_3)_2]N^i\text{-}Pr\}_2YCH(SiMe_3)_2$ (**3**) approximately perpendicular to the Y, C(27), Si(5), Si(6) plane. The isopropyl and methyl groups on the guanidinate ligands as well as the hydrogen atoms have been omitted for clarity. Thermal ellipsoids are drawn at 30% probability.

Table 3. Selected Bond Distances [Å] and Angles [deg] for $[(Me_3Si)_2NC(N^iPr)_2]_2YCH(SiMe_3)_2$ (3)

Distances			
Y−N(1)	2.373(2)	Si(6)−C(32)	1.869(3)
Y−N(2)	2.305(2)	Si(6)−C(33)	1.854(4)
Y−N(5)	2.372(2)	Si(6)−C(27)	1.826(4)
Y−N(4)	2.374(2)	N(1)−C(7)	1.333(3)
Y−C(27)	2.402(3)	N(2)−C(7)	1.342(3)
Si(5)−C(27)	1.831(3)	N(3)−C(7)	1.437(3)
Si(5)−C(28)	1.851(5)	N(4)−C(20)	1.341(3)
Si(5)−C(29)	1.831(3)	N(5)−C(20)	1.338(3)
Si(5)−C(30)	1.813(4)	N(6)−C(20)	1.441(3)
Si(6)−C(31)	1.883(3)		

Angles			
N(2)−Y−N(5)	106.63(8)	Si(2)−N(3)−Si(1)	122.48(13)
N(2)−Y−N(1)	57.47(7)	C(20)−N(4)−C(14)	120.5(2)
N(5)−Y−N(1)	150.99(7)	C(20)−N(4)−Y	94.22(15)
N(2)−Y−N(4)	115.08(7)	C(14)−N(4)−Y	144.98(16)
N(5)−Y−N(4)	56.72(7)	C(20)−N(5)−C(17)	121.0(2)
N(1)−Y−N(4)	105.25(7)	C(20)−N(5)−Y	94.39(15)
N(2)−Y−C(27)	116.20(11)	C(17)−N(5)−Y	144.32(17)
N(5)−Y−C(27)	100.94(13)	C(20)−N(6)−Si(3)	118.45(17)
N(1)−Y−C(27)	107.89(13)	C(20)−N(6)−Si(4)	117.53(17)
N(4)−Y−C(27)	128.15(11)	Si(3)−N(6)−Si(4)	124.00(12)
C(27)−Y−C(7)	114.84(12)	N(1)−C(7)−N(2)	114.5(2)
C(27)−Y−C(20)	116.75(13)	N(1)−C(7)−N(3)	123.0(2)
C(7)−Y−C(20)	127.80(7)	N(2)−C(7)−N(3)	122.5(2)
C(7)−N(1)−C(1)	121.5(2)	N(3)−C(7)−Y	178.04(19)
C(7)−N(1)−Y	92.60(15)	N(5)−C(20)−N(4)	114.6(2)
C(1)−N(1)−Y	145.44(19)	N(5)−C(20)−N(6)	122.4(2)
C(7)−N(2)−C(4)	121.7(2)	N(4)−C(20)−N(6)	123.0(2)
C(7)−N(2)−Y	95.38(16)	N(6)−C(20)−Y	176.75(18)
C(4)−N(2)−Y	142.80(16)	Si(6)−C(27)−Si(5)	116.99(17)
C(7)−N(3)−Si(2)	118.70(17)	Si(6)−C(27)−Y	108.97(15)
C(7)−N(3)−Si(1)	118.82(17)	Si(5)−C(27)−Y	133.16(18)

Y center with bite angles of 57.47(7)° and 56.72(7)°. This results in an approximately C_2 symmetric molecular geometry in which the pseudo 2-fold axis lies along the Y−C(27) bond.

Characteristically, the hydrocarbyl carbon is nearly planar (deviation from the Si(5), Si(6), Y plane by less than 0.1 Å).[14] The shorter bond distance between yttrium and the hydrocarbyl carbon (C(27)−Y = 2.402-

(13) Den Haan, K. H.; Wielstra, Y.; Eshius, J. J. W.; Teuben, J. H. *J. Organomet. Chem.* **1987**, *323*, 181.

(3) Å) compared to [*p*-$MeOC_6H_4C(NSiMe_3)_2]_2YCH(SiMe_3)_2$ (2.431(5) Å)[6a] and Cp_2*$YCH(SiMe_3)_2$ (2.468(7) Å)[11] may suggest a more electron-deficient yttrium center or a sterically less encumbered guanidinate complex.

Examination of the hydrocarbyl ligand in **3** reveals a clear asymmetry in the Y−C−Si angles (108.97° vs 133.16°) (Figure 3). This contrasts with benzamidinate complex [*p*-$MeOC_6H_4C(NSiMe_3)_2]_2YCH(SiMe_3)_2$, which exhibited identical angles of 115°.[6a] Similar but slightly more severe distortions have been observed in lanthanide systems,[15,16] in Cp*$Y(OC_6H_3{}^tBu_2)$ $CH(SiMe_3)_2$,[17] and in $Cp^*_2YCH(SiMe_3)_2$.[11] In these complexes the origin of this distortion was attributed to an agostic interaction between the Lewis acidic metal and the β-SiC and γ-CH σ bonds. In the case of **3** the methyl carbon that comes in closest proximity to the Y center is C(31) at a distance of 3.237 Å. For comparison the closest β-methyl carbon in Cp*$YCH(SiMe_3)_2$ was located 2.878 Å from the Y center. A slight lengthening of the Si(6)−C(31) bond length (1.883(3) Å) compared to the other Si−Cmethyl within the hydrocarbyl ligand (average = 1.844 Å) is consistent with such an interaction.

Structure, bonding, and angular parameters obtained from a single crystal study of complex **5** are presented in Figure 4 and Table 4, respectively. In this case the $\{[(SiMe_3)_2NC(N^iPr)_2]_2Y(\mu\text{-}Me_2\}^-$ portion of the structure is conveniently described as having a distorted pseudo-octahedral geometry defined by the four nitrogen atoms of the two chelating bidentate guanidinate ligands and the two methyl groups. Closely associated with this moiety, through coordination to the μ-Me groups, is a Li cation coordinated to the two N centers of a TMEDA.

The guandinate ligands and the Me groups in **5** exhibit symmetrical coordination. The guanidinates coordinate to Y to form planar cycles and exhibited four Y−N distances that are identical within error (2.399(3)−2.412(3) Å). The bite angles of the two ligands are identical at 55.36(10)°.

The $Y-C_{methyl}$ distances of 2.505(4) and 2.508(4) Å are equal and are comparable to those in Cp*Y[PhC$(NSiMe_3)_2]Me_2Li$(TMEDA) (2.480(3), 2.493(3) Å).[6b] These distances are 0.1 Å longer than the Y−C bond in **3** (2.402(3) Å) presumably due to the bridging bonding mode for the methyl groups in **5**. For example, the bridging Y−C distances in dimeric $[Cp_2Y(\mu\text{-}Me)]_2$ are 2.552(10) Å,[18] while the terminal Y−C distance of 2.468(7) Å is observed in Cp*$YCH(SiMe_3)_2$.[11] The Me−Y−Me angle of 91.22(12)° is similar to the analogous angle in Cp*Y[PhC$(NSiMe_3)_2]Me_2Li$(TMEDA) (89.67(11)°)[6b] and relaxed relative to the Cl−Y−Cl angles in **2** of 76°.

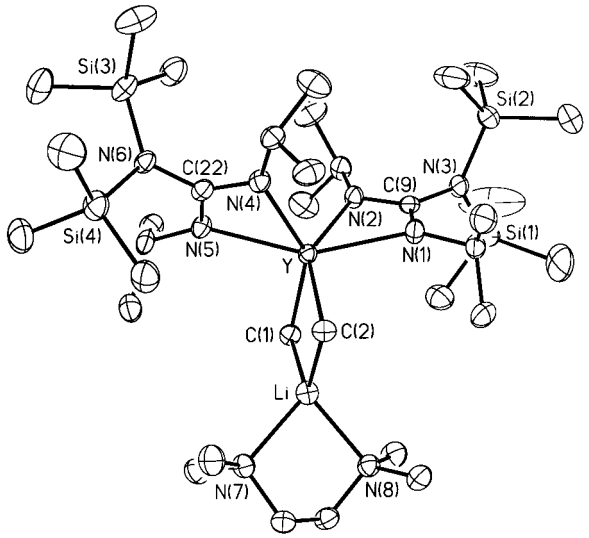

Figure 4. Molecular structure of $\{^iPrNC[N(SiMe_3)_2]N^iPr\}_2Y(\mu\text{-}Me)_2Li[Me_2NCH_2CH_2NMe_2]$ (**5**). Hydrogen atoms have been omitted for clarity. Thermal ellipsoids are drawn at 30% probability.

Table 4. Selected Bond Distances [Å] and Angles [deg] for $[(Me_3Si)_2NC(N^iPr)_2]_2Y(\mu\text{-}Me)_2Li$[TMEDA] (5)

	Distances		
Y−N(4)	2.399(3)	Li−N(8)	2.184(7)
Y−N(2)	2.402(3)	N(1)−C(9)	1.324(5)
Y−N(5)	2.410(3)	N(2)−C(9)	1.342(4)
Y−N(1)	2.412(3)	N(3)−C(9)	1.450(5)
Y−C(1)	2.505(4)	N(3)−Si(1)	1.744(3)
Y−C(2)	2.508(4)	N(3)−Si(2)	1.745(4)
Y−C(22)	2.844(4)	N(4)−C(22)	1.327(4)
Y−C(9)	2.851(4)	N(5)−C(22)	1.329(4)
Y−Li	3.074(7)	N(6)−C(22)	1.449(4)
Li−N(7)	2.143(8)		
	Angles		
N(4)−Y−N(2)	106.54(11)	C(3)−N(1)−Y	141.9(3)
N(4)−Y−N(5)	55.36(10)	C(9)−N(2)−C(6)	122.7(3)
N(2)−Y−N(5)	106.42(11)	C(9)−N(2)−Y	94.9(2)
N(4)−Y−N(1)	107.66(11)	C(6)−N(2)−Y	142.1(2)
N(2)−Y−N(1)	55.36(10)	C(9)−N(3)−Si(1)	117.3(3)
N(5)−Y−N(1)	153.37(11)	C(9)−N(3)−Si(2)	119.0(2)
N(4)−Y−C(1)	145.66(11)	Si(1)−N(3)−Si(2)	123.67(19)
N(2)−Y−C(1)	91.00(12)	C(22)−N(4)−C(16)	122.2(3)
N(5)−Y−C(1)	91.75(11)	C(22)−N(4)−Y	95.2(2)
N(1)−Y−C(1)	106.60(11)	C(16)−N(4)−Y	142.5(2)
N(4)−Y−C(2)	90.21(11)	C(22)−N(5)−C(19)	122.4(3)
N(2)−Y−C(2)	145.73(11)	C(22)−N(5)−Y	94.6(2)
N(5)−Y−C(2)	107.68(12)	C(19)−N(5)−Y	142.3(2)
N(1)−Y−C(2)	91.39(12)	C(22)−N(6)−Si(4)	118.7(2)
C(1)−Y−C(2)	91.22(12)	C(22)−N(6)−Si(3)	118.5(3)
C(1)−Y−C(22)	118.60(12)	Si(4)−N(6)−Si(3)	122.80(17)
C(2)−Y−C(22)	98.48(11)	N(1)−C(9)−N(2)	114.1(3)
C(1)−Y−C(9)	97.90(12)	N(1)−C(9)−N(3)	123.2(3)
C(2)−Y−C(9)	118.11(12)	N(2)−C(9)−N(3)	122.7(4)
C(22)−Y−C(9)	127.63(11)	N(4)−C(22)−N(5)	114.6(3)
N(7)−Li−N(8)	85.8(3)	N(4)−C(22)−N(6)	123.2(3)
C(9)−N(1)−C(3)	122.0(3)	N(5)−C(22)−N(6)	122.2(3)
C(9)−N(1)−Y	95.0(2)	N(6)−C(22)−Y	173.9(3)

Definitive formulation of the structural features of complex **6** was provided by single-crystal X-ray diffraction analysis (Figure 5, Table 5).[19] Consistent with our proposals, the structural analysis of **6** revealed a mononuclear species with the coordination sphere of the

(14) (a) Schumann, H.; Rosenthal, E. C. E.; Kociok-Kohn, G.; Molander, G. A.; Winterfeld, J. *J. Organomet. Chem.* **1995**, *496*, 233. (b) Clark, D. L.; Gordon, J. C.; Huffman, J. C.; Watkin, J. G.; Zwick, B. D. *Organometallics* **1994**, *13*, 4266. (c) Giardello, M. A.; Conticello, V. P.; Brard, L.; Sabat, M.; Rheingold, A. L.; Stern, C. L.; Marks, T. J. *J. Am. Chem. Soc.* **1994**, *116*, 10212. (d) Conticello, V. P.; Brard, L.; Giardello, M. A.; Tsuji, Y.; Sabat, M.; Stern, C. L.; Marks T. J. *J. Am. Chem. Soc.* **1992**, *114*, 2761. (e) Hitchcock, P. B.; Lappert, M. F.; Smith, R. G. *J. Chem. Soc., Chem. Comm.* **1989**, 369. (f) Hitchcock, P. B.; Lappert, M. F.; Smith, R. G.; Bartlett, R. A.; Power, P. P. *J. Chem. Soc., Chem. Commun.* **1988**, 1007.

(15) Jeske, G.; Lauke, H.; Mauermann, H.; Swepston, P. N.; Schumann, H.; Marks, T. J. *J. Am. Chem. Soc.*, **1985**, *107*, 8091. Heeres, H. J.; Renkema, J.; Booij, M.; Meetsma, A.; Teuben, J. H. *Organometallics* **1988**, *7*, 2495. Jeske, G.; Schock, L. E.; Swepston, P. N.; Schumann, H.; Marks, T. J. *J. Am. Chem. Soc.* **1985**, *107*, 8103. Stern, D.; Sabat, M.; Marks, T. J. *J. Am. Chem. Soc.* **1990**, *112*, 9558.

(16) Schaverien, C. J *Adv. Organomet. Chem.* **1994**, *36*, 283. Schaverien, C. J.; Nesbitt, G. J. *J. Chem. Soc., Dalton Trans.* **1992**, 157.

(17) Klooster, W. T.; Brammer, L.; Schaverien, C. J.; Budzelaar, P. H. M. *J. Am. Chem. Soc.* **1999**, *121*, 1381.

(18) Holton, J.; Lappert, M. F.; Ballard, D. G. H.; Pearce, R.; Atwood, J. L.; Hunter, W. E. *J. Chem. Soc., Dalton Trans.* **1979**, 54.

Definitive formulation of the structural features of complex **6** was provided by single-crystal X-ray diffraction analysis (Figure 5, Table 5).[19] Consistent with our proposals, the structural analysis of **6** revealed a mononuclear species with the coordination sphere of the

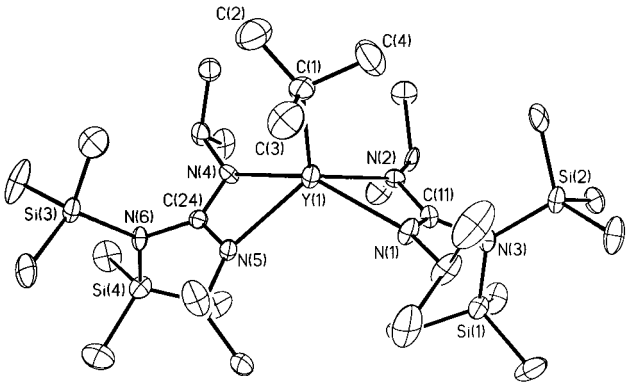

Figure 5. Molecular structure showing one of the two symmetry unique molecules of $^{i}PrNC[N(SiMe_3)_2]N^{i}Pr\}_2YC(CH_3)_3$ (**6**). Hydrogen atoms have been omitted for clarity. Thermal ellipsoids are drawn at 30% probability.

Table 5. Selected Bond Distances [Å] and Angles [deg] for $[(Me_3Si)_2NC(N^{i}Pr)_2]_2YC(CH_3)_3$ (6)

Distances			
Y(1)−N(5)	2.328(9)	N(2)−C(8)	1.442(12)
Y(1)−N(2)	2.330(9)	N(3)−C(11)	1.461(10)
Y(1)−C(1)	2.332(9)	N(4)−C(24)	1.310(11)
Y(1)−N(4)	2.359(9)	N(4)−C(18)	1.482(13)
Y(1)−N(1)	2.409(9)	N(5)−C(24)	1.343(12)
Y(1)−C(24)	2.768(6)	N(5)−C(21)	1.459(13)
Y(1)−C(11)	2.770(6)	N(6)−C(24)	1.422(10)
N(1)−C(11)	1.289(12)	N(6)−Si(4)	1.752(9)
N(1)−C(5)	1.429(13)	N(6)−Si(3)	1.755(9)
N(2)−C(11)	1.376(12)		

Angles			
N(5)−Y(1)−N(2)	125.2(3)	C(5)−N(1)−Y(1)	145.4(8)
N(5)−Y(1)−C(1)	116.7(3)	C(11)−N(2)−C(8)	123.8(9)
N(2)−Y(1)−C(1)	118.1(3)	C(11)−N(2)−Y(1)	93.1(5)
N(5)−Y(1)−N(4)	56.7(3)	C(8)−N(2)−Y(1)	142.9(7)
N(2)−Y(1)−N(4)	102.2(3)	C(11)−N(3)−Si(1)	115.4(7)
C(1)−Y(1)−N(4)	112.7(3)	C(11)−N(3)−Si(2)	118.2(7)
N(5)−Y(1)−N(1)	107.8(3)	Si(1)−N(3)−Si(2)	126.4(6)
N(2)−Y(1)−N(1)	57.4(3)	C(24)−N(4)−C(18)	120.8(10)
C(1)−Y(1)−N(1)	103.5(3)	C(24)−N(4)−Y(1)	93.6(6)
N(4)−Y(1)−N(1)	143.7(3)	C(18)−N(4)−Y(1)	141.5(8)
N(5)−Y(1)−C(24)	28.9(3)	C(24)−N(5)−C(21)	122.6(10)
N(2)−Y(1)−C(24)	119.8(3)	C(24)−N(5)−Y(1)	94.1(6)
C(1)−Y(1)−C(24)	114.56(17)	C(21)−N(5)−Y(1)	142.7(8)
N(4)−Y(1)−C(24)	28.2(3)	C(24)−N(6)−Si(4)	120.4(7)
N(1)−Y(1)−C(24)	132.1(3)	C(24)−N(6)−Si(3)	114.3(7)
N(5)−Y(1)−C(11)	118.8(3)	Si(4)−N(6)−Si(3)	125.2(6)
N(2)−Y(1)−C(11)	29.7(3)	N(4)−C(24)−N(5)	113.9(8)
C(1)−Y(1)−C(11)	114.42(18)	N(4)−C(24)−N(6)	123.7(10)
N(4)−Y(1)−C(11)	125.5(3)	N(5)−C(24)−N(6)	121.3(10)
N(1)−Y(1)−C(11)	27.7(3)	N(1)−C(11)−N(2)	117.4(7)
C(24)−Y(1)−C(11)	131.0(3)	N(1)−C(11)−N(3)	123.1(10)
C(11)−N(1)−C(5)	122.6(10)	N(2)−C(11)−N(3)	119.3(9)
C(11)−N(1)−Y(1)	91.9(6)		

Y(III) center composed of the four nitrogen atoms of two chelating guanidinate anions and the ^{t}Bu group. Like complex **3**, the coordination geometry of **6** is best described as trigonal planar, with the bisector of the guanidinate ligands (Y−C(11) and Y−C(24) vectors) defining two vertexes and the alkyl carbon (C(1)) the third. The angles defined by these vectors sum to 360°. This analysis emphasizes that fact that the molecular structure of **6** resembles that of the bent metallocene derivatives containing Cp_2M units.

(19) For conciseness, the discussion of the structural parameters of **6**, the thermal ellipsoid plot shown in Figure 5, and the data in Table 5 are confined to one of the two molecules that constitute the asymmetric unit in the crystal structure. Full crystallographic data are provided in the Supporting Information.

In contrast to the hydrocarbyl ligand in **3**, the angles around C(1) are regular and fall in the range 111.1(4)−114.0(4)° with no structural evidence for an agostic interaction. The Y−C(butyl) distance of 2.332(9) Å is shorter than the Y−C bond in **3** (2.402(3) Å), a feature that is presumably a reflection of the relative steric congestion for these groups.

The two nitrogens and bridging carbon atoms for each of the two guanidinate ligands (N(1)−C(11)−N(2) and N(4)−C(24)−N(5)) lie in a plane that includes the Y atom. Interestingly, the bonding parameters within the guanidinate ligands in **6** differ from each other. The N(1)−C(11)−N(2) moiety shows evidence of a localized π system (N(1)−C(11) 1.289(12) Å, N(2)−C(11) 1.376(12) Å), while the ligand defined by N(4)−C(24)−N(5) exhibits more symmetrical bond lengths (N(4)−C(24) 1.310(11) Å, N(5)−C(24) 1.343(12) Å) indicative of a more delocalized π system. In combination with the long Y(1)−N(1) distance (2.409(9) Å) when compared with the other Y−N distances in **6** (Y(1)−N(2) 2.330(9) Å, Y(1)−N(4) 2.359(9) Å, Y(1)−N(5) 2.328(9) Å), these observations are consistent with a significant contribution from a localized resonance structure **A**. The dihedral angles formed by the planar $N(SiMe_3)_2$ function and the YNCN plane average 83.8°, which excludes significant π overlap between these moieties.

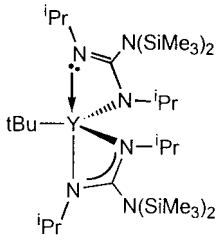

A

Conclusion

In summary, guanidinate ligands have proven to be useful in the preparation of a family of bis(guanidinate)-yttrium complexes. A combination of X-ray crystallographic and spectroscopic studies confirm the approximate C_2 symmetric features of the bis(guanidinate) compounds. The preparations of complexes **3**, **5**, and **6** support the fact that **2** represents a novel precursor for soluble organometallic complexes of yttrium that are free of cyclopentadienyl ligands. The orientation of the lone pair of electrons on the planar $N(SiMe_3)_2$ groups of the guanidinate ligands indicates that no conjugation occurs between these substituents and the guanidinate NCN π system. The use of these complexes to yield catalytically active species is currently under investigation. Along with this effort, our continuing investigations are oriented at further investigating the steric and electronic features that influence the reactivity of transition metal guanidinate compounds.

Experimental Section

General Considerations. All manipulations were performed either in a nitrogen-filled Vacuum Atmospheres glovebox with a high-capacity recirculator or using standard Schlenk-line techniques under nitrogen. Diethyl ether, hexane, THF, and toluene were sparged with nitrogen and then dried by passage through a column of activated alumina using an

apparatus purchased from Anhydrous Engineering. Pentane and deuterated solvents were dried with Na/K alloy. Anhydrous yttrium trichloride (beads), MeLi (1.4 M in diethyl ether), and ^{t}BuLi (1.7 M in pentane) were purchased from Aldrich and used without further purification. ^{1}H and ^{13}CNMR spectra were recorded on either a Gemini 200 MHz or a Bruker AMX 500 MHz spectrometer and referenced to the residual protons in the solvent. All elemental analyses were run on a Perkin-Elmer PE CHN 4000 elemental analysis system.

{[(Me$_3$Si)$_2$NC(NCHMe$_2$)$_2$]$_2$Y(μ-Cl)}$_2$ (2). To a solution of in situ generated **1** (5.87 g, 20 mmol) in 60 mL ether was added YCl_3 (1.95 g, 10 mmol). The reaction mixture was stirred for 2 days and evaporated to dryness in vacuo. The yellow residue was extracted with hexane and filtered to remove LiCl. The filtrate was concentrated and cooled to −30 °C. White powder of **2** was obtained in two crops (5.08 g, 3.65 mmol, 73%). Colorless crystals, suitable for X-ray analysis, could be obtained from hexane, ether, or toluene. ^{1}H NMR (benzene-d_6, ppm): 3.86 (m, 8H, C*H*Me$_2$), 1.52 (d, 24H, (C*H*$_3$)$_2$CH, $^3J_{H-H}$ = 6.2 Hz), 1.49 (d, 24H, (C*H*$_3$)$_2$CH, $^3J_{H-H}$ = 6.2 Hz), 0.35 (br s, 72H, Si(C*H*$_3$)$_3$). ^{13}C NMR (benzene-d_6, ppm): 171.09 (*C*N$_3$), 46.81(*C*HMe$_2$), 28.63, 27.56 ((*C*H$_3$)$_2$CH), 3.41(CN(Si(*C*H$_3$)$_3$)$_2$). Anal. Calcd (found) for $C_{52}H_{128}N_{12}Si_8Cl_2Y_2$: C, 44.77 (44.42); H, 9.25 (9.36); N, 12.05 (11.97).

[(Me$_3$Si)$_2$NC(NCHMe$_2$)$_2$]$_2$YCH(SiMe$_3$)$_2$ (3). A Schlenk flask was charged with **2** (1.39 g, 1.0 mmol) and diethyl ether (60 mL). The solution was cooled to −78 °C, and LiCH(SiMe$_3$)$_2$ (0.33 g, 2.0 mmol) was added. The mixture was slowly warmed to room temperature and stirred for 3 h. After removal of volatiles under vacuum, the residue was extracted with hexane. Filtration, concentration, and cooling to −30 °C gave **3** as colorless, cube-shaped crystals (1.32 g, 1.61 mmol, 80%). ^{1}H NMR (benzene-d_6, ppm): 3.85 (m, 4H, C*H*Me$_2$), 1.31 (d, 24H, (C*H*$_3$)$_2$CH, $^3J_{H-H}$ = 6.4 Hz), 0.50 (s,18H, CH(Si(C*H*$_3$)$_3$)$_2$), 0.25 (s, 36H, NCN(Si(C*H*$_3$)$_3$)$_2$), −1.11 (br, 1H, C*H*(SiMe$_3$)$_2$). ^{13}C NMR (benzene-d_6, ppm): 170.70 (*C*N$_3$), 46.84 (*C*HMe$_2$), 41.33 (d, *C*H(Si(CH$_3$)$_3$)$_2$, J_{Y-C} = 33 Hz), 28.03 ((*C*H$_3$)$_2$CH), 6.62 (CH-(Si(*C*H$_3$)$_3$)$_2$), 3.14 (CN(Si(*C*H$_3$)$_2$)). Anal. Calcd (found) for $C_{33}H_{83}N_6Si_6Y$: C, 48.25 (48.32); H, 10.18(10.41); N, 10.23 (10.20).

[(Me$_3$Si)$_2$NC(NCHMe$_2$)$_2$]$_2$YN(SiMe$_3$)$_2$ (4). Following a procedure similar to the synthesis of **3**, complex **4** was prepared by treating **2** (0.70 g, 0.5 mmol) with LiN(SiMe$_3$)$_2$ (0.17 g, 1.0 mmol). Recrystallization from hexane yielded colorless crystals (0.72 g, 0.88 mmol, 88%). ^{1}H NMR (benzene-d_6, ppm): 3.85 (m, 4H,C*H*Me$_2$), 1.31 (d, 24H,(C*H*$_3$)$_2$CH, $^3J_{H-H}$ = 6.4 Hz), 0.50 (s, 18H, YN(Si(C*H*$_3$)$_3$)$_2$), 0.27 (s, 36H,CN(Si(C*H*$_3$)$_3$)$_2$). ^{13}C NMR (benzene-d_6, ppm): 170.03 (*C*N$_3$), 46.79 (*C*HMe$_2$), 27.93 ((*C*H$_3$)$_2$-CH), 6.27 (N(Si(*C*H$_3$)$_3$)$_2$), 3.35 (CN(Si(*C*H$_3$)$_3$)$_2$. Anal. Calcd (found) for $C_{32}H_{82}N_7Si_6Y$: C, 46.73 (46.62); H, 10.05 (9.70); N, 11.92 (11.80).

[(Me$_3$Si)$_2$NC(NCHMe$_2$)$_2$]$_2$Y(μ-Me)$_2$Li[Me$_2$NCH$_2$CH$_2$-NMe$_2$] (5). A Schlenk flask was charged with **2** (0.98 g, 0.7 mmol) and TMEDA (0.22 mL, 1.4 mmol) and 60 mL of hexane. The solution was cooled to −78 °C, and methyllithium (2 mL, 2.8 mmol) was added to the stirring solution. The mixture was allowed to warm slowly to room temperature and to stir for 1 h. After filtration, concentration and cooling of the filtrate to −30 °C yielded colorless crystals of **5** (0.89 g, 1.1 mmol, 79%). ^{1}H NMR (benzene-d_6, ppm): 3.94 (m, 4H, C*H*Me$_2$), 1.92 (s, 12H, TMEDA-Me), 1.62 (br, 4H,TMEDA-CH$_2$), 1.39 (d, 24H, (C*H*$_3$)$_2$CH, $^3J_{H-H}$ = 6.2 Hz), 0.34 (s, 36H, CN(Si(C*H*$_3$)$_3$)$_2$), −0.65 (br, 6H, μ-Me). ^{13}C NMR (benzene-d_6, ppm): 167.77 (*C*N$_3$), 56.93 (TMEDA-CH$_2$), 46.48 (*C*HMe$_2$), 46.25 (TMEDA-Me), 27.69 ((*C*H$_3$)$_2$CH), 11.80 (br,μ-Me), 2.91 (CN(Si(*C*H$_3$)$_3$)$_2$). Anal. Calcd (found) for $C_{34}H_{86}N_8Si_4YLi$: C, 50.09 (49.89); H, 10.68 (10.37); N, 13.74 (14.02).

[(Me$_3$Si)$_2$NC(NCHMe$_2$)$_2$]$_2$YCMe$_3$ (6). To a stirring solution of **2** (1.18 g, 0.85 mmol) in diethyl ether was added LiC(CH$_3$)$_3$ (1 mL, 1.7 mmol). After filtration to remove LiCl and removal of reaction solvent, crude **6** was isolated as a yellow powder (0.86 g, 1.19 mmol, 70%). Crystals suitable for X-ray analysis could be obtained from pentane at −30 °C. ^{1}H NMR (benzene-d_6, ppm): 3.85 (m, 4H, C*H*Me$_2$), 1.43 (s, 9H, C(C*H*$_3$)$_3$, 1.35 (d, 12H, (C*H*$_3$)$_2$CH, $^3J_{H-H}$ = 6.4 Hz), 1.27 (d, 12H, (C*H*$_3$)$_2$CH, $^3J_{H-H}$ = 6.4 Hz), 0.27 (s, 18H, CN(Si(C*H*$_3$)$_3$)$_2$), 0.24 (s, 18H, CN(Si-(C*H*$_3$)$_3$)$_2$). ^{13}C NMR (benzene-d_6, ppm): 168.8 (*C*N$_3$), 46.5 (*C*HMe$_2$), 39.9 (d, *C*Me$_3$,$^1J_{Y-C}$ = 46 Hz), 30.60 (C(*C*H$_3$)$_3$), 27.50, 27.15 ((*C*H$_3$)$_2$CH), 2.51, 2.41 (CN(Si(*C*H$_3$)$_3$)$_2$). Anal. Calcd (found) for $C_{30}H_{73}N_6Si_4Y$: C, 50.10 (49.85); H, 10.23 (10.37); N, 11.69 (11.88).

X-ray Structural Determinations of 2, 3, 5, and 6. Single crystals were mounted on thin glass fibers using viscous oil and then cooled to the data collection temperature. Crystal data and details of the measurements are summarized in Table 1. Data were collected on a Bruker AX SMART 1k CCD diffractometer using 0.3° ω-scans at 0, 90, and 180° in ϕ. Unit-cell parameters were determined from 60 data frames collected at different sections of the Ewald sphere. Semiempirical absorption corrections based on equivalent reflections were applied.

The structures were solved by direct methods, completed with difference Fourier syntheses, and refined with full-matrix least-squares procedures based on F^2. In the case of **5**, the penultimate difference Fourier map showed several peaks of a possibly severely disordered solvent molecule, located away from the compound molecule, which could not be refined as a chemically reasonable solvent and were assigned carbon atom identities with refined partial site occupancies.

All non-hydrogen atoms were refined with anisotropic displacement parameters. All hydrogen atoms were treated as idealized contributions. All scattering factors and anomalous dispersion factors are contained in the SHELXTL 5.1 program library.

Acknowledgment. This work was supported by the Natural Sciences and Engineering Research Council of Canada.

Supporting Information Available: A thermal ellipsoid plot for [(Me$_3$Si)$_2$NC(N^{i}Pr)$_2$]$_2$Y(μ-Cl)$_2$Li(THF)$_2$. Fully labeled structural diagrams for compounds **2**, **3**, **5**, and **6**. X-ray crystallographic files in CIF format for the structure determinations of **2**, **3**, **5**, and **6**. This material is available free of charge via the Internet at http://pubs.acs.org.

OM0009029